Journal of Alloys and Compounds 616 (2014) 208–212

Contents lists available at ScienceDirect

Journal of Alloys and Compounds

journal homepage: www.elsevier.com/locate/jalcom

Comparison of ethanol sensitivity based on cobalt–indium combined oxide nanotubes and nanofibers

Changbai Liu [a,*], Xiao Chi [b], Xingyi Liu [a], Shenglei Wang [a]

[a] College of Electronic Science & Engineering, Jilin University, Changchun 130012, PR China
[b] State Key Laboratory of Superhard Materials, College of Physics, Jilin University, Changchun 130012, PR China

ARTICLE INFO

Article history:
Received 26 April 2014
Received in revised form 11 July 2014
Accepted 14 July 2014
Available online 22 July 2014

Keywords:
Indium oxide
Cobalt
Semiconductor
Gas sensor
Nanotubes

ABSTRACT

Nano sized semiconductor oxide type gas sensor has been widely studied due to its high sensitivity. Therein, one-dimensional nanostructures have attracted a lot of interests. In this work, nanofiber and nanotube of one-dimensional nano sized cobalt–indium combined oxide were fabricated by single nozzle electrospinning. The ethanol gas sensing properties of Co–In oxide nanofiber and nanotube were investigated. The morphologies were observed by scanning electron microscopy (SEM). The elementary composition was characterized by powder X-ray diffraction (XRD), and energy-dispersive X-ray spectrometry (EDS). The BET surface area of the nanotube can be calculated to be 22 m^2/g, which is larger than 18 m^2/g of nanofiber. The results reveal that one-dimensional nanotubes have larger sensitivity to ethanol than that of one-dimensional nanofibers. Besides, the comparison of their response and recovery curves was tested. The selectivity was also investigated. Both nanofibers and nanotubes show a fast response and excellent selectivity.

1. Introduction

With the progress of technology and the development of industry, the demand for environmental monitoring is more and more urgent. Hence, semiconductor oxide based gas sensors has been attracting the increasing attentions for the advantages of low cost, easy fabrication, high sensitivity and convenience [1,2]. Structure of the semiconductor oxides has an important effect upon the gas sensing properties. Recent years, many successful one-dimensional nanostructures of WO_3, Fe_2O_3, ZnO, SnO_2 and In_2O_3 have been fabricated and demonstrated good gas sensitivities [3–7].

Semiconductor oxides obtained from electrospinning benefit from large specific surface areas and fast transmission of charge carrier by the one-dimensional nanostructure [8,9]. Several years earlier, lots of works about electrospinning technique had been reported and demonstrated that electrospinning is an effective and convenient method to synthesize one-dimensional material [10,11]. In recent years, lots of works focused on synthesis of combined semiconductor oxides by electrospinning, which often contain two kinds of different metal cation [12–14]. Electrospinning technique is difficult to explore new morphologies compared with some other traditional methods such as hydrothermal method. To the majority of single nozzle electrospinning, the final synthetic products are nanowires, nanotube, string of beads or some other special morphologies, which are often prepared by changing the ratio of the precursor solution and the annealing process [15,16]. However, string of beads nanostructure is usually judged as a flaw. Under the same fiber diameter, string of beads nanostructure possesses smaller specific surface areas than those of nanofiber, which probably has a negative effect for gas sensing sensitivity. From the previous research achievements of single nozzle electrospinning, the hollow structure of nanotubes fabricated by single nozzle electrospinning are usually has a relative larger diameter than that of nanofiber [11,17–19]. However, their gas sensing properties are seldom investigated together.

The gas sensing properties were significantly improved for porous, hollow, hierarchical and interconnected nanostructures, especially for hollow nanostructures semiconductors [20–22]. With this aim, eletrospinning technique is employed to synthesize the cobalt–indium combined oxide nanofiber and nanotubes via the same precursor solution. The obtained two kinds of one-dimensional nanostructure are compared in terms of their structures, specific surface areas and their gas sensing properties. Hollow structure really has a positive effect on gas sensitivity.

* Corresponding author. Tel./fax: +86 431 8502260.
E-mail address: liwei99@jlu.edu.cn (C. Liu).

http://dx.doi.org/10.1016/j.jallcom.2014.07.112
0925-8388/

2. Experimental

2.1. Chemical reagents and preparation of the sensing materials

Ethanol (⩾99.5%), N,N-dimethylformamide (DMF, ⩾99.9%), indium nitrate hydrate (⩾99.99%) and cobalt nitrate hexahydrate (⩾99.99%) were purchased from Aladdin (China). Polyvinyl pyrrolidone (PVP, Mw = 1,300,000) was purchased from Sigma–Aldrich (U.S.A.).

Cobalt–indium combined oxide of nanofibers and nanotubes were synthesized as follows. $In(NO_3)_3$ (0.42 g) and $Co(NO_3)_2{\cdot}6H_2O$ (0.004 g) were mixed with 4 g of DMF and 4 g of absolute ethanol under magnetic stirring for 30 min. Meanwhile, 4 g of absolute ethanol and 1 g of PVP were mixed with a separate container under magnetic stirring. The above solutions were then mixed and stirred vigorously for 10 h to obtain the precursor solution. In a typical electrospinning process, the precursor solution was injected by a syringe and an aluminum foil as the collector. The distance between the syringe (anode) and the collector (cathode) was 20 cm and the voltage was supplied with 15 kV. Then the composite fibers in the form of non-woven mats were collected and annealed at 500 °C for 2 h at the heating rate of 2 °C/min and 10 °C/min, respectively.

2.2. Characterizations

The morphologies of the products were recorded by scanning electron microscopy (SEM) using a FEI XL30ESEM instrument. Powder X-ray diffraction (XRD) patterns were obtained on a SHIMADZU XRD-6000 with Cu Kα1 radiation (λ = 0.15406 nm). Energy-dispersive X-ray spectrometry (EDS) patterns were obtained on an FEI XL30ESEM–FEG system. Nitrogen adsorption was operated on a Micromeritics ASAP 2420 apparatus.

2.3. Sensor fabrication and gas sensor measurement

The detailed process of sensor fabrication based on the products has been described in our previous work [23]. Briefly, the sensing paste containing Co–In combined oxides and deionized water (weight ratio is 4:1) was coated onto the ceramic tube with a pair of gold electrodes was previously printed. A Ni–Cr heating wire was inserted into the ceramic tube to provide operating temperature.

The gas sensing properties of the cobalt–indium combined oxide were measured using a CGS-8 gas sensing analysis system (Beijing Elite Tech Co., China). The sensitivity of sensors was measured in a sealed test chamber. In order to test different concentration target gases, target gases were diluted with air at different ratios. The sensor response is defined as R_a/R_g, where R_a is the resistance in pure air and R_g is the resistance in the target gas. The response and recovery times are defined as the time taken by the sensor to reach 90% of the total resistance variation for adsorption and desorption, respectively [24]. The experiments was operated at 25 °C and the relative humidity was about 40%.

3. Results and discussion

3.1. Structural and morphological characteristics

The morphologies of products after annealing are shown in Fig. 1. Fig. 1a and b shows the products annealed at the heating rate of 2 °C/min. Fig. 1c and d show the products annealed at the heating rate of 10 °C/min, respectively. As shown in Fig. 1a and b, the cobalt–indium combined oxide nanofibers are irregularly distributed. The diameter of nanofibers are substantially uniform, which is about 50–90 nm. In Fig. 1b, it is clear to observe that the surface of nanofiber is smooth. Fig. 1c and d shows the morphologies of cobalt–indium combined oxide nanotubes in low and high magnification, respectively. The distribution of nanotubes is also random. Compare with nanofibers, nanotubes present a lager diameter of about 150–200 nm and the surface of nanotubes are full of wrinkles. There are also some nanopores present on the nanotube surface, which may benefit to gas sensing properties.

The powder X-ray diffraction (XRD) patterns were recorded and presented in Fig. 2. All of the prominent diffraction peaks of both samples are agree with cubic structure of single-crystal In_2O_3 (JCPDS 71-2195), without any impure peak, indicating that both of the products are of high purity. The contents of Co are so low that cannot be found in XRD patterns.

In order to confirm the presence of Co, which cannot be found in XRD patterns, EDS patterns of cobaltindium combined oxide are presented in Fig. 3. These patterns confirmed that elements of In, Co, C and O were present in products. The products were capped with Au before EDX characteristics and there is evidence of Au in Fig. 3. The element of C probably came from the substrate and the incomplete calcination of PVP.

To analyze the pore size distribution of nanotube and compare two kinds of products specific surface area, nitrogen adsorption and desorption dynamic curves and pore size distribution curve were recorded and the results are shown in Fig. 4. Patterns of nanofiber and nanotube are shown in Fig. 4a and b, respectively. The BET surface areas of nanofiber and nanotube are 18 and 22 m^2/g, respectively. The pore size distribution curve of nanotube is

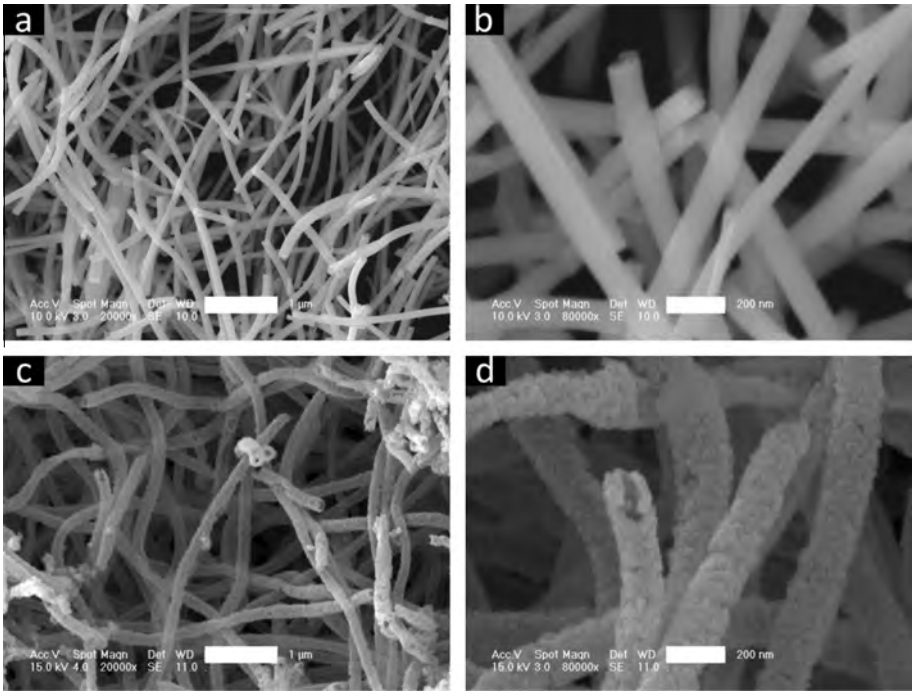

Fig. 1. SEM images of cobalt–indium combined oxide: (a and b) nanofiber; (c and d) nanotube.

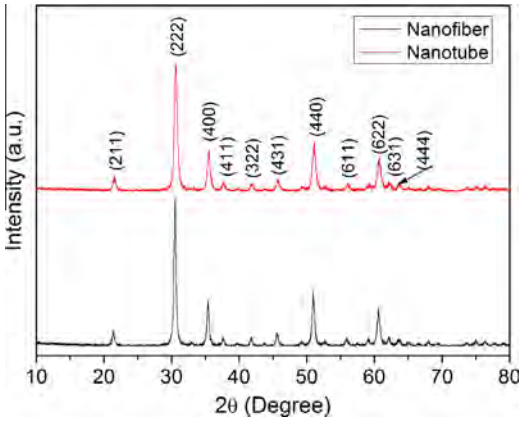

Fig. 2. XRD patterns of nanofiber and nanotube, respectively.

inserted into Fig. 4b. The pore size distribution dynamic curve fluctuated heavily at low pore diameter, which may be attributed to the nanopore irregularly distribute on the surface of nanotube. These results reveal that nanotube may exhibit high gas sensing properties [25,26].

3.2. Gas-sensing properties

Many researchers have revealed that semiconductor oxide mixed with some metal cations can enhance the gas sensing properties. For example, An et al. obtained Au–In_2O_3 nanotube by template method and investigated their ethanol sensitivity [27]. Zhang et al. also demonstrated that ZnO–In_2O_3 nanofiber exhibit an outstanding ethanol sensing property [28]. In this work, we prepared cobalt–indium combined oxide nanofiber and nanotube and their ethanol gas sensing properties were investigated.

The relationships between the temperature and response of two gas sensors to 100 ppm ethanol are presented in Fig. 5. The two tendencies of responses are both increase with increasing temperature and reach their maximum at 260 °C, and then decrease rapidly with increasing temperature. The sensor based on cobalt–indium combined oxide nanofiber shows a relatively low response

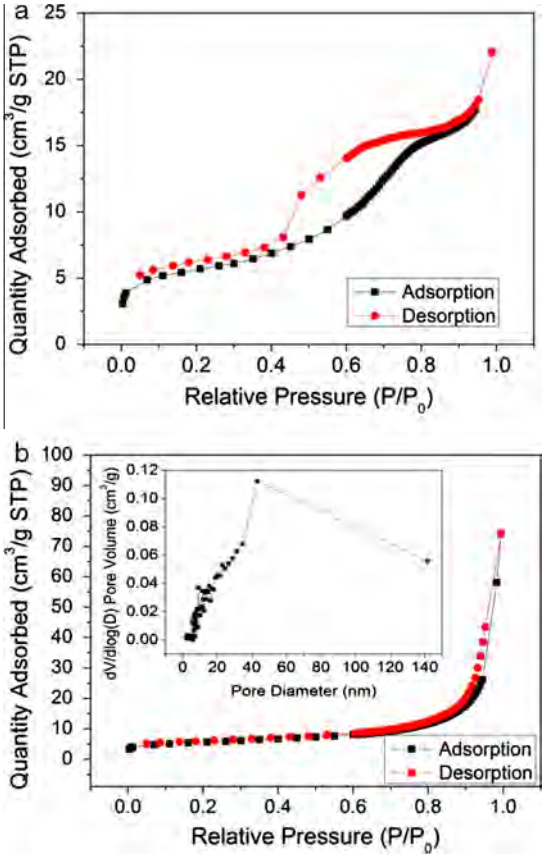

Fig. 4. N_2 adsorption–desorption isotherm of (a) nanofiber and (b) nanotube; pore size distribution plots (inset into (b) of nanotube.

at the temperature of 230–280 °C, and the maximum is 41.5 at 260 °C. The sensor based on cobalt–indium combined oxide nanotubes exhibit the larger response of 93.1 at 260 °C. 260 °C was chosen as the working temperature for the further experiments. This phenomenon can be ascribed to the balance of oxygen

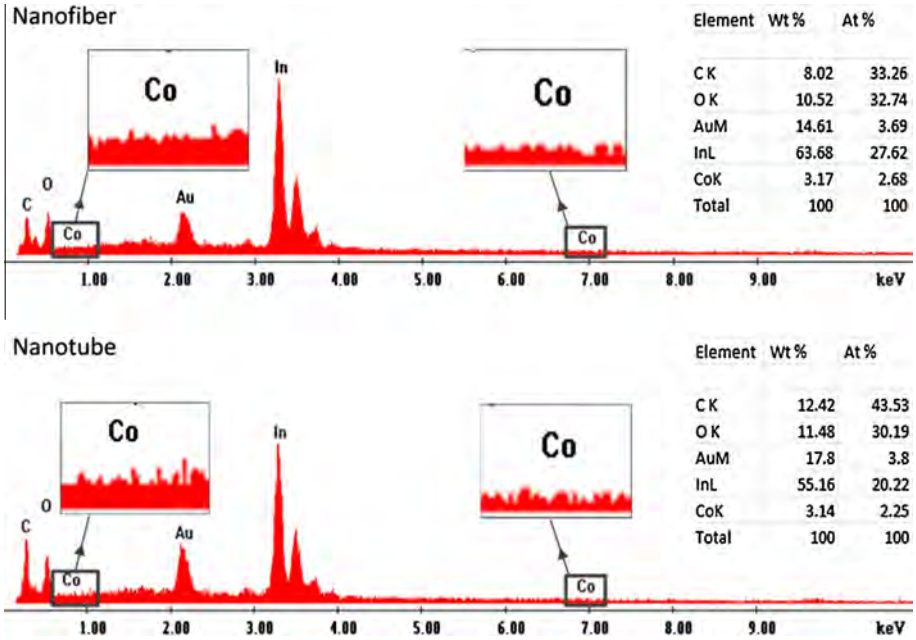

Fig. 3. EDS patterns of nanofiber and nanotube, respectively.

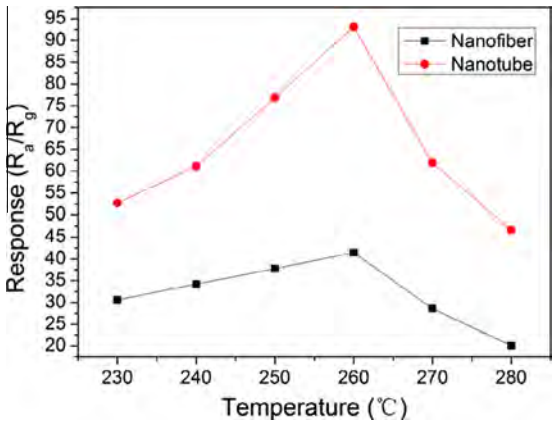

Fig. 5. Responses of sensors based on nanofiber and nanotube to 100 ppm ethanol at different temperature, respectively.

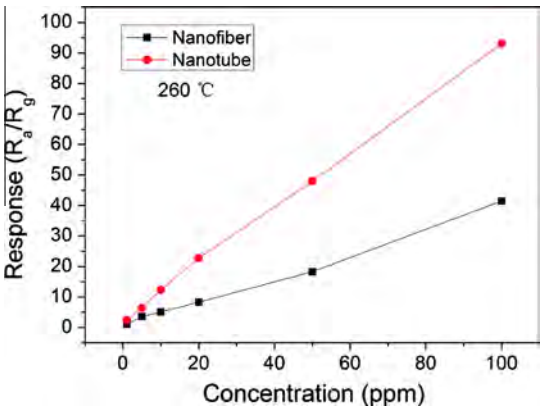

Fig. 7. The response of nanofibers and nanotubes sensors to 1–100 ppm ethanol at 260 °C.

adsorption and desorption reaction on the samples surface [29]. At low temperature, with the temperature increasing the response value is increased for the formation of oxygen ion. At high temperature, with the temperature increasing the response value decreased is ascribed to the increase of desorption reaction.

In previous works, the sensitivities of ethanol gas sensors based on CuO–In_2O_3 [30], SnO_2–Fe_2O_3 [31], Au–ZnO [32] and TiO_2–Co_3O_4 [33] to 100 ppm ethanol are about 4.7, 16, 16 and 40, respectively. In our work, the sensor based on cobalt–indium combined oxide nanotubes is about 93, which show the prior response to ethanol. The results reveal that cobalt–indium combined oxide nanotubes sensor have a good sensitivity to ethanol.

The dynamic curves of response and recovery times based on nanofiber and nanotube to 100 ppm ethanol are presented in Fig. 6. The dynamic curves of response and resistance are shown in Fig. 6a and b, respectively. When the sensor was exposed in ethanol gas, the resistance decrease rapidly and tend to be stable. When the sensor was put back and exposed in air, the resistance gradually increases and reaches the initial value. The response times based on nanofiber and nanotube were both about 3 s. The recovery times based on nanofiber are 25 s, which was shorter than that of based on nanotube (72 s). Compare with nanofibers sensor, these results indicate that nanotubes sensor possesses the higher response, however, also possesses the slower recovery times. This phenomenon may be due to that the structures of plicated nanotubes have negative effect on ethanol gas release from tubular structure.

To further test the sensitivity of nanofiber and nanotube, their sensors were exposed to ethanol with different concentration at 260 °C. The sensors were exposed in 1–100 ppm ethanol and the responses were recorded in Fig. 7. Sensor based on nanotubes exhibit higher response in each concentration than that of nanofibers sensor. The results also reveal that the nanotubes sensor can detect ethanol even down to 1 ppm with response of 2.5, which is an acceptable value for detection.

The selective test of sensors based on nanofibers and nanotubes towards 100 ppm ethanol, acetone, formaldehyde, toluene, hydrogen and carbon monoxide are operated at 260 °C. In Fig. 8, both of the nanofibers and nanotubes sensors show excellent selectivity to ethanol. Their ethanol sensitivities are far higher than that of other gases. Distinguishing ethanol and acetone is usually difficult for their similar chemical nature [34]. Interestingly, in this work, ethanol and acetone can be easily distinguished at the same concentrations.

3.3. Gas sensing mechanism

It is deserved to note that the cobalt–indium combined oxide nanotubes sensor shows an excellent sensitivity to ethanol, which is about double times larger than that of cobalt–indium combined oxide nanofibers sensor. The synthesis of nanofiber and nanotube are come from the same non-woven mats. The structure of the nanotube is one-dimensional hollow structure, which has large surface areas. Besides, the pores irregularly distributed on the surface of nanotube are beneficial to the diffusion and adsorption of target gas. However, the gas was difficult to diffuse from the

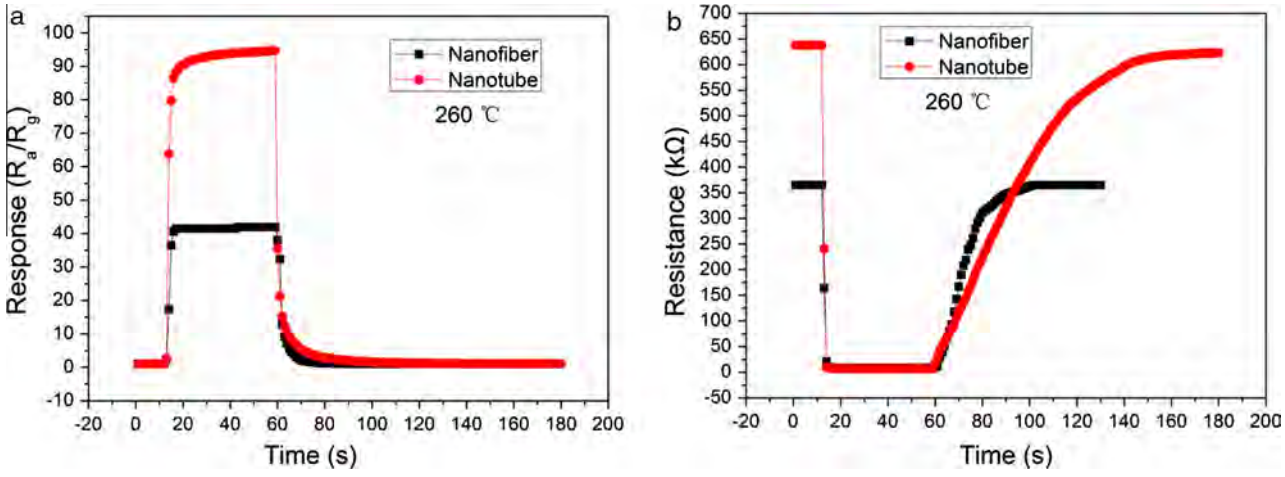

Fig. 6. Dynamic curves of 100 ppm ethanol based on (a) response and (b) resistance of nanofibers and nanotubes sensors at 260 °C.

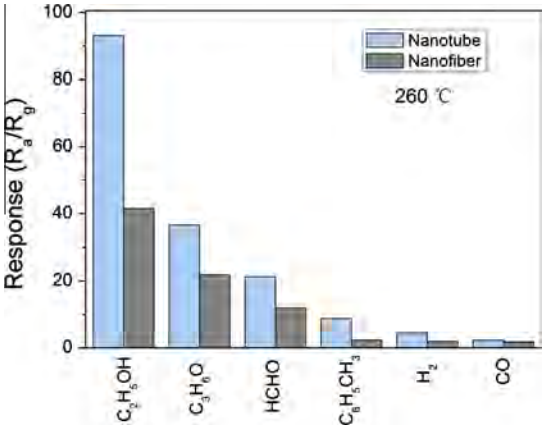

Fig. 8. The response of nanofibers and nanotubes sensors to 100 ppm different gases at 260 °C.

inner nanotube of the nanotube. Moreover, the larger change ratio of resistances may also have negative effect on response and recovery, which lead to a slower response and recovery.

The products contained cobalt–indium combined oxide, where indium oxide plays a principal effect on sensing property. The slight mixing of cobalt oxide can form the heterojunction at the interface between the two oxides. Such a formation of cobalt oxide (p-type)–indium oxide (n-type) heterojunction is also important for the high sensitivity to ethanol at 260 °C. The depletion layer formed at the interface, and then enhances the resistance in air of the sensor [35]. Therefore, when the sensor is exposed in target gas, the ratio of resistance variation changes a lot. As a result, the cobalt–indium combined oxide sensors show a good sensitivity.

As a semiconductor resistance sensor, cobalt–indium combined oxide sensor also exhibits an inherent mechanism which was previously reported. When sensor is put in air at working temperature, the surrounding oxygen molecules are attached to the surface of sensing material and capture free electrons. Then, the oxygen molecules are ionized to O_2^-, O^-, and O^{2-}. The depletion layer is formed. The loss of electrons results in the enhancement of resistance. When the sensor is exposed in the ethanol atmosphere, the oxygen ion will release electrons back. Hence, the resistance decreases [29,36].

4. Conclusions

In summary, two kinds of one-dimensional nano sized cobalt–indium combined oxide were fabricated by single nozzle electrospinning and their ethanol gas sensing properties were investigated. Cobalt–indium combined oxide of nanofiber and nanotube both showed good sensitivity, response times and selectivity to ethanol. When comparison was made between them, nanotube shows the higher response and slower recovery. These results exhibit the significance of the fabricated one-dimensional nanomaterial structures for gas sensing application.

Acknowledgements

The work has been supported by competition funded projects of "challenge cup" college students' extracurricular academic science and technology works (450060497053).

References

[1] P. Sun, Y. Cai, S. Du, X. Xu, L. You, J. Ma, F. Liu, X. Liang, Y. Sun, G. Lu, Sens. Actuat., B 182 (2013) 336–343.
[2] J. Su, X.-X. Zou, Y.-C. Zou, G.-D. Li, P.-P. Wang, J.-S. Chen, Inorg. Chem. 52 (2013) 5924–5930.
[3] S. An, S. Park, H. Ko, C. Lee, Ceram. Int. 40 (2014) 1423–1429.
[4] C. Zhao, W. Hu, Z. Zhang, J. Zhou, X. Pan, E. Xie, Sens. Actuat., B 195 (2014) 486–493.
[5] Y. Abdi, S.M. Jebreiil Khadem, P. Afzali, Curr. Appl. Phys. 14 (2014) 227–231.
[6] S. Park, S. An, S. Park, C. Jin, W.I. Lee, C. Lee, Appl. Phys. A 110 (2012) 471–477.
[7] P. Song, Q. Wang, Z. Yang, Sens. Actuat., B 168 (2012) 421–428.
[8] Z. Li, Y. Fan, J. Zhan, Eur. J. Inorg. Chem 2010 (2010) 3348–3353.
[9] W.Q. Li, S.Y. Ma, Y.F. Li, X.B. Li, C.Y. Wang, X.H. Yang, L. Cheng, Y.Z. Mao, J. Luo, D.J. Gengzang, G.X. Wan, X.L. Xu, J. Alloys Comp. 605 (2014) 80–88.
[10] D.-J. Yang, I. Kamienchick, D.Y. Youn, A. Rothschild, I.-D. Kim, Adv. Funct. Mater. 20 (2010) 4258–4264.
[11] J.-A. Park, J. Moon, S.-J. Lee, S.H. Kim, H.Y. Chu, T. Zyung, Sens. Actuat., B 145 (2010) 592–595.
[12] A. Katoch, S.-W. Choi, G.-J. Sun, H.W. Kim, S.S. Kim, Nanotechnology 25 (2014) 175501.
[13] G.X. Wan, S.Y. Ma, X.B. Li, F.M. Li, H.Q. Bian, L.P. Zhang, W.Q. Li, Mater. Lett. 114 (2014) 103–106.
[14] C. Zhu, Y. Li, Q. Su, B. Lu, J. Pan, J. Zhang, E. Xie, W. Lan, J. Alloys Comp. 575 (2013) 333–338.
[15] Z. Zhang, X. Li, C. Wang, L. Wei, Y. Liu, C. Shao, J. Phys. Chem. C 113 (2009) 19397–19403.
[16] S. Wei, M. Zhou, W. Du, Sens. Actuat., B 160 (2011) 753–759.
[17] X. Yu, F. Song, B. Zhai, C. Zheng, Y. Wang, Physica E 52 (2013) 92–96.
[18] Y. Liu, C. Gao, X. Pan, X. An, Y. Xie, M. Zhou, J. Song, H. Zhang, Z. Liu, Q. Zhao, Y. Zhang, E. Xie, Appl. Surf. Sci. 257 (2011) 2264–2268.
[19] A. Stafiniak, B. Boratyński, A. Baranowska-Korczyc, A. Szyszka, M. Ramiączek-Krasowska, J. Prażmowska, K. Fronc, D. Elbaum, R. Paszkiewicz, M. Tłaczała, Sens. Actuat., B 160 (2011) 1413–1418.
[20] J. Zhu, K.Y.S. Ng, D. Deng, ACS Appl. Mater. Inter. 6 (2014) 2996–3001.
[21] D. Wang, S. Du, X. Zhou, B. Wang, J. Ma, P. Sun, Y. Sun, G. Lu, Cryst. Eng. Commun. 15 (2013) 7438.
[22] L. Gan, C. Wu, Y. Tan, B. Chi, J. Pu, L. Jian, J. Alloys Comp. 585 (2014) 729–733.
[23] X. Chi, C. Liu, L. Liu, S. Li, H. Li, X. Zhang, X. Bo, H. Shan, Mater. Sci. Semicond. Process. 18 (2014) 160–164.
[24] L. Liu, Y. Zhang, G. Wang, S. Li, L. Wang, Y. Han, X. Jiang, A. Wei, Sens. Actuat., B 160 (2011) 448–454.
[25] J. Huang, Y. Dai, C. Gu, Y. Sun, J. Liu, J. Alloys Comp. 575 (2013) 115–122.
[26] H. Shan, C. Liu, L. Liu, L. Wang, S. Li, X. Zhang, X. Bo, X. Chi, Sci. China Chem. 56 (2013) 1722–1726.
[27] S. An, S. Park, H. Ko, C. Jin, W.I. Lee, C. Lee, J. Phys. Chem. Solids 74 (2013) 979–984.
[28] X.-J. Zhang, G.-J. Qiao, Appl. Surf. Sci. 258 (2012) 6643–6647.
[29] S.K. Lim, S.-H. Hwang, D. Chang, S. Kim, Sens. Actuat., B 149 (2010) 28–33.
[30] S. Park, H. Ko, S. An, W.I. Lee, S. Lee, C. Lee, Ceram. Int. 39 (2013) 5255–5262.
[31] P. Sun, X. Zhou, C. Wang, K. Shimanoe, G. Lu, N. Yamazoe, J. Mater. Chem. A 2 (2014) 1302.
[32] N.S. Ramgir, M. Kaur, P.K. Sharma, N. Datta, S. Kailasaganapathi, S. Bhattacharya, A.K. Debnath, D.K. Aswal, S.K. Gupta, Sens. Actuat., B 187 (2013) 313–318.
[33] Y.Q. Liang, Z.D. Cui, S.L. Zhu, Z.Y. Li, X.J. Yang, Y.J. Chen, J.M. Ma, Nanoscale 5 (2013) 10916.
[34] Z. Wang, Z. Li, L. Liu, X. Xu, H. Zhang, W. Wang, W. Zheng, C. Wang, J. Am. Ceram. Soc. 93 (2010) 634–637.
[35] H.-J. Lee, J.-H. Song, Y.-S. Yoon, T.-S. Kim, K.-J. Kim, W.-K. Choi, Sens. Actuat., B 79 (2001) 200–205.
[36] L. Wang, H. Dou, F. Li, J. Deng, Z. Lou, T. Zhang, Sens. Actuat., B 183 (2013) 467–473.